Inorganica Chimica Acta, 120 (1986) 135–143

Interaction between FeRu Bimetallic Carbonyl Clusters and Oxide Supports. II. Decomposition and Thermal Behaviour on Hydrated Alumina

S. DOBOS, I. BÖSZÖRMÉNYI, J. MINK and L. GUCZI

Institute of Isotopes of the Hungarian Academy of Sciences, H-1525 Budapest, P.O. Box 77, Hungary

(Received April 15, 1986)

Abstract

As known, on hydrated alumina support the $Ru_3(CO)_{12}$ cluster quickly decomposes into monometallic subcarbonyls. By FT-IR spectroscopy combined with data handling procedures, the structure and thermal behaviour of the bimetallic systems of $Fe_2Ru(CO)_{12}/Al_2O_3$ and $H_2FeRu_3(CO)_{13}$ together with that of $Ru_3(CO)_{12}$ have been studied. At the end of an interaction with the hydrated alumina surface, iron–ruthenium bimetallic clusters decompose into identical ruthenium anchored surface species $Ru_A = Ru^{III}(CO)_2$, $Ru_B = Ru^{II}(CO)_2$ and $Ru_C = Ru^0(CO)_2$, like pure ruthenium clusters, and no CO bonded to iron has been detected Ru_B and Ru_C are stable in a wide temperature range (300–500 K) and they can be interconverted by oxidation and reduction. Ru_A is less stable (300–400 K). These main molecule-like species, anchored onto uniform sites of the surface, are accompanied by mobile subcarbonyls and stable monocarbonylic species, which occupy a large variety of different sites.

Introduction

In Part I of this series it was shown that after impregnation at least two types of M–CO bonds occurred on the surface [1]. However, the method used in Part I did not allow us to answer the question whether different metal–carbonyl bondings belonged to one or more different surface species. The aim of the present paper, together with Part III, is to gain detailed structural infomation about the surface subcarbonyls.

Recently, we reported that $Fe_2Ru(CO)_{12}$ and $H_2FeRu_3(CO)_{13}$ clusters supported on alumina after impregnation and a standard 12 h drying process *in vacuo* yielded surface species of similar spectra with five main bands: 2140(w), 2070(s), 2050(sh), 2001(m) and 1970(sh) cm^{-1}. Due to this similarity we suggested that on hydrated alumina the original cluster framework collapsed and ruthenium subcarbonyl species were formed because the above bands were also characteristic of subcarbonyls originated from $Ru_3(CO)_3$ [2]. Several recent investigations provided convincing evidences that, depending on the conditions, more or less five CO stretching frequencies appeared in the infrared spectra during the interaction of $Ru_3(CO)_{12}$ with hydrated alumina [3–5].

Three surface species were assumed to be responsible for the five bands but these species were interpreted in different ways. Kuznetzov *et al.* [3] assigned the band pair at 2050 and 1970 cm^{-1} to the surface structure of $[Ru(CO)_2X_2]_n$ while the three bands at 2140, 2070 and 2000 cm^{-1} were represented by the structures $[Ru(CO)_3X_2]_n$ and $[Ru(CO)_4X_2]_n$.

Knözinger *et al.* divided the five bands into three pairs of bands: 2140 and 2070, 2070 and 2000, 2050 and 1970 cm^{-1} and assigned them to the surface species of $Ru(CO)_3{}^{II}$, $Ru(CO)_2{}^{II}$ and $Ru^0(CO)_2$, respectively [4].

Zecchina *et al.* arranged the bands in the same three pairs with the assignments to the species $Ru^{III}(CO)_2$, $Ru^{II}(CO)_2$ and $Ru^0(CO)_2$, respectively [5]. This last assignment has been experimentally extremely well supported and we have chosen it as a basic point. On the other hand, in our first attempt to prove or disprove the existence of the above three structures by a quantitative preliminary data analysis in the case of Ru_3/Al_2O_3 system, we concluded that as the ratio of the relative intensities of the bands at 2050 and 1970 cm^{-1} was constant under different conditions, they certainly represented a well defined stable species $[Ru^0(CO)_2]$ over a wide temperature range. However, the other three bands at 2140, 2070 and 2000 cm^{-1} could not be characterized by only two structures which remained unchanged over a rather wide temperature range because no strict correlation was found between their relative intensities [6]. Therefore, we have reinvestigated the Ru_3/Al_2O_3 system using different approaches in order to deconvolute the additional spectral features from the band system and to gain more information about the five main features, too. By thoroughly investigating the Fe_2Ru/Al_2O_3 and H_2FeRu_3/Al_2O_3 systems and by carefully examining spectral developments, we have attempted to spot

0020-1693/86/$3.50

a manifold analogy of these systems to that of Ru_3/Al_2O_3. In order to enhance spectral features we have used data handling procedures like substraction of spectra and calculation of the first and second derivatives of the spectra.

Experimental

Materials and Sample Preparation

The support was Degussa Alon C Al_2O_3 (SA = 100 m^2/g), heated *in vacuo* at 573 K for 12 h then contacted with the pentane solution of the cluster compound. $Ru_3(CO)_{12}$ (ICN Pharmaceutical) and $Fe_3(CO)_{12}$ (STREM Chemicals) were used without purification. The method given in ref. 7 was applied to produce $Fe_2Ru(CO)_{12}$ and $H_2FeRu_3(CO)_{13}$. Calculated metal loadings were about 1%. The supported clusters were dried under vacuum overnight and pressed into wafers (10–20 mg/cm^2) which were then placed in a heatable conventional vacuum IR cell.

Infrared spectra, under vacuum or H_2 stream were recorded at temperatures ranging from 303 K to 693 K using a DIGILAB FTS-20C spectrometer equipped with a Nova 3 computer. For all spectra reported a 200 scans data accumulation was carried out at resolution = 4 cm^{-1}. Fully decarbonylated samples were used as references.

Data Handling

All double beam spectra were baseline corrected. Difference spectra were obtained using substraction procedures between two spectra taken at two different temperatures. First and second derivatives were computed by consecutive numerical derivations of the baseline-corrected experimental spectra. For analysing the spectra the sum of maximum 10 Gaussians was fitted to the data points. Numerical integration over the entire CO stretching region was performed using the sum of the areas of theoretical trapezoids formed by successive pairs of data points above the zero baseline.

Results

One of the most notable facts we experienced was that $Fe_3(CO)_{12}$ at the end of the 12 h drying process was found to be completely decomposed, that means no measurable CO could be detected.

Baseline-corrected spectra of the systems Ru_3/Al_2O_3/vacuum, (abbreviated form for $Ru_3(CO)_{12}/Al_2O_3$ is Ru_3/Al_2O_3, etc.) Fe_2Ru/Al_2O_3/vacuum and H_2FeRu_3/Al_2O_3/ vacuum are shown in Fig. 1(a), (b) and (c), while those of the systems $Ru_3/Al_2O_3/H_2$, $Fe_2Ru/Al_2O_3/H_2$ and $H_2FeRu_3/Al_2O_3/H_2$ in Fig. 2(a), (b) and (c) respectively.

The first derivatives are collected in Fig. 3(a), (b) and (c); the second derivatives in Fig. 4(a), (b) and

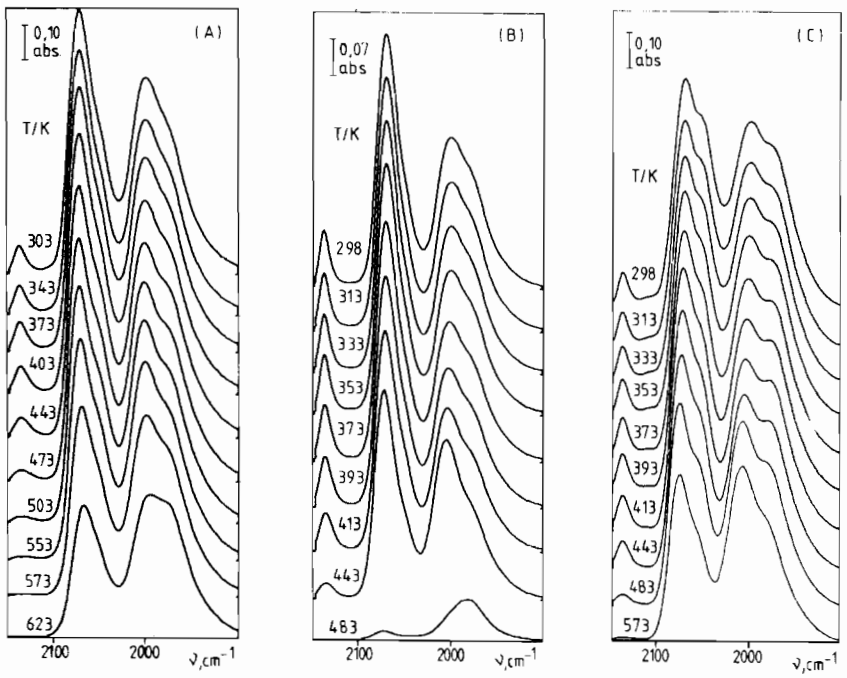

Fig. 1. Baseline-corrected spectra of the systems (a) Ru_3/Al_2O_3/vacuum; (b) Fe_2Ru/Al_2O_3/vacuum and (c) H_2FeRu_3/Al_2O_3/vacuum.

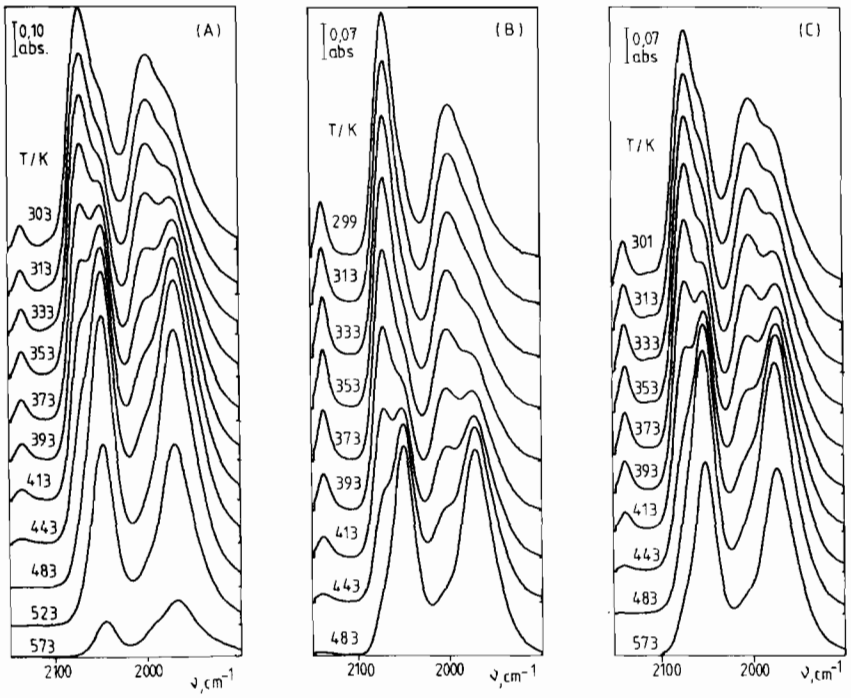

Fig. 2. Baseline-corrected spectra of the systems (a) $Ru_3/Al_2O_3/H_2$; (b) $Fe_2Ru/Al_2O_3/H_2$ and (c) $H_2FeRu_3/Al_2O_3/H_2$.

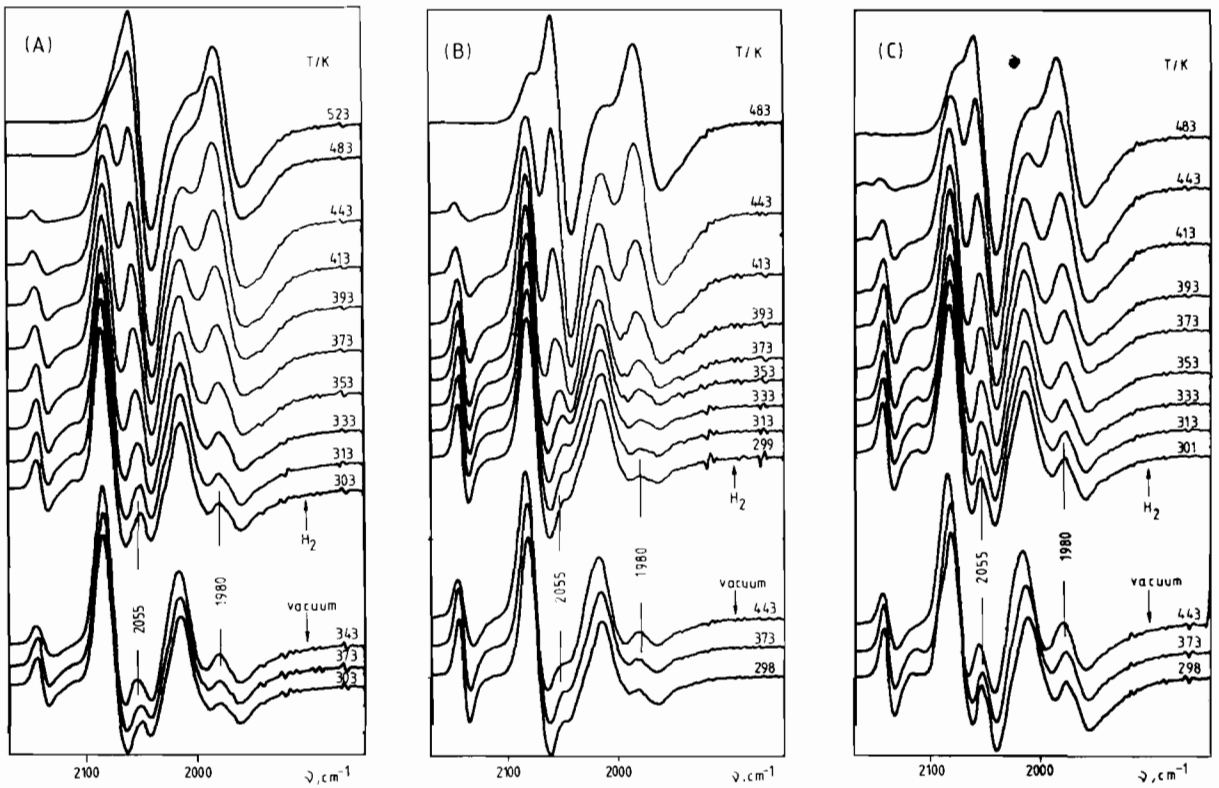

Fig. 3. First derivative spectra of the systems (a) Ru_3/Al_2O_3/vacuum and H_2; (b) Fe_2Ru/Al_2O_3/vacuum and H_2; (c) H_2FeRu_3/Al_2O_3/vacuum and H_2.

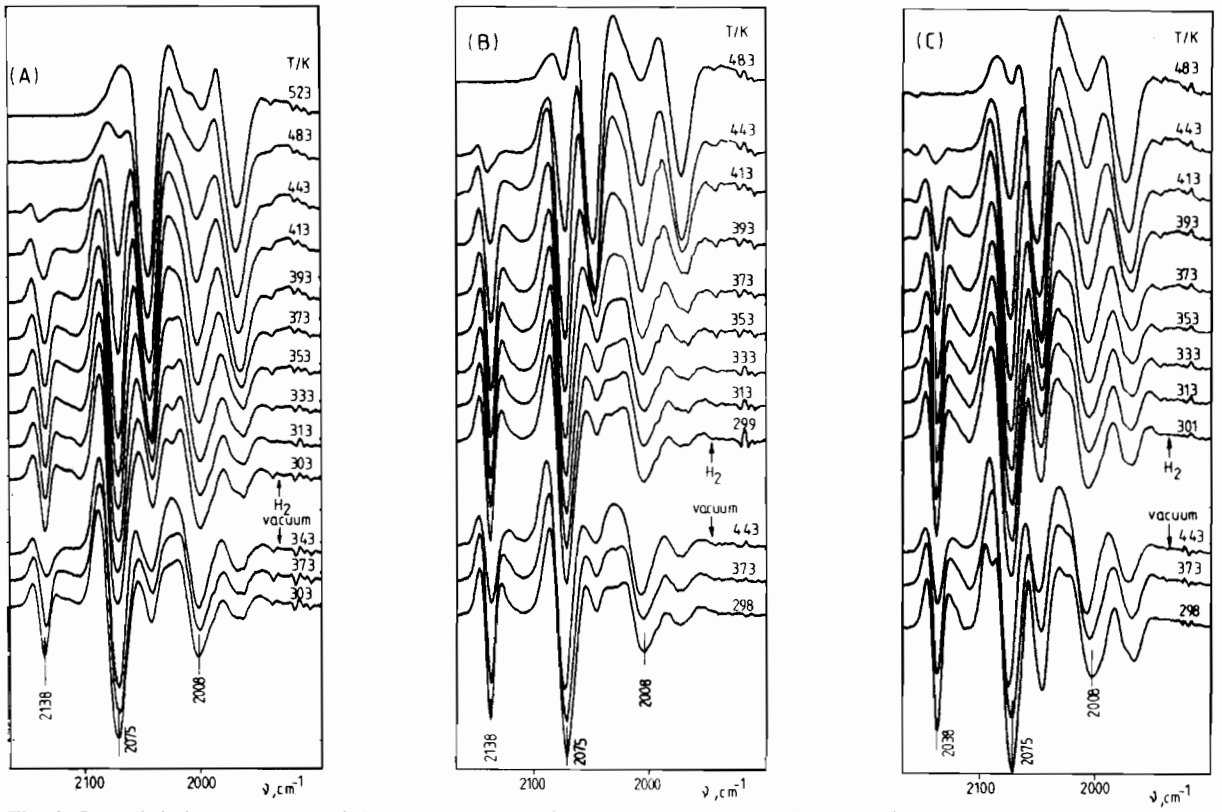

Fig. 4. Second derivative spectra of the systems (a) Ru_3/Al_2O_3 vacuum and H_2; (b) Fe_2Ru/Al_2O_3 vacuum and H_2 and (c) H_2-$FeRu_3/Al_2O_3$ vacuum and H_2.

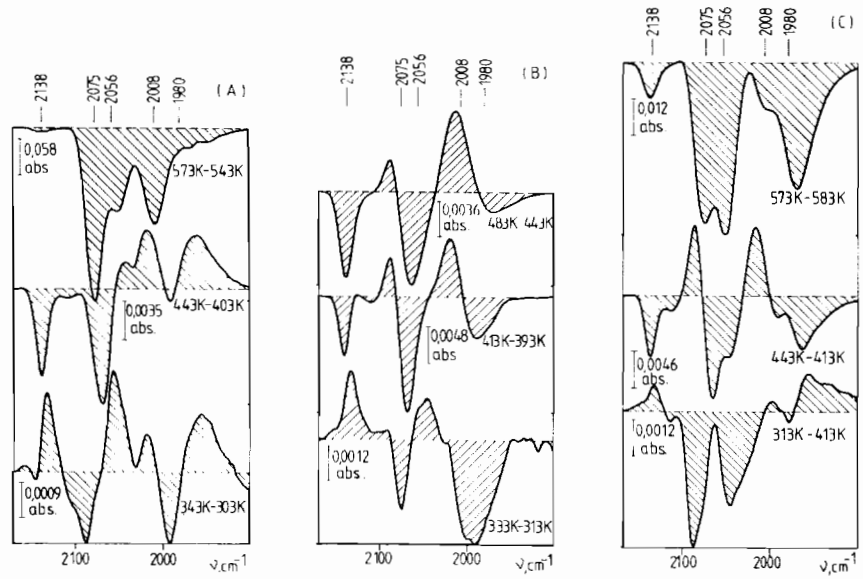

Fig. 5. Characteristic difference spectra of the systems (a) Ru_3/Al_2O_3/vacuum; (b) Fe_2Ru/Al_2O_3 vacuum and (c) H_2FeRu_3/Al_2O_3/vacuum.

(c). Owing to the quite high quality of the original experimental spectra it was not necessary to perform a smoothing procedure before derivation.

Figure 5(a)–(c) and Fig. 6(a)–(c) show some characteristic difference spectra. Each spectrum was calculated from two spectra by substracting the

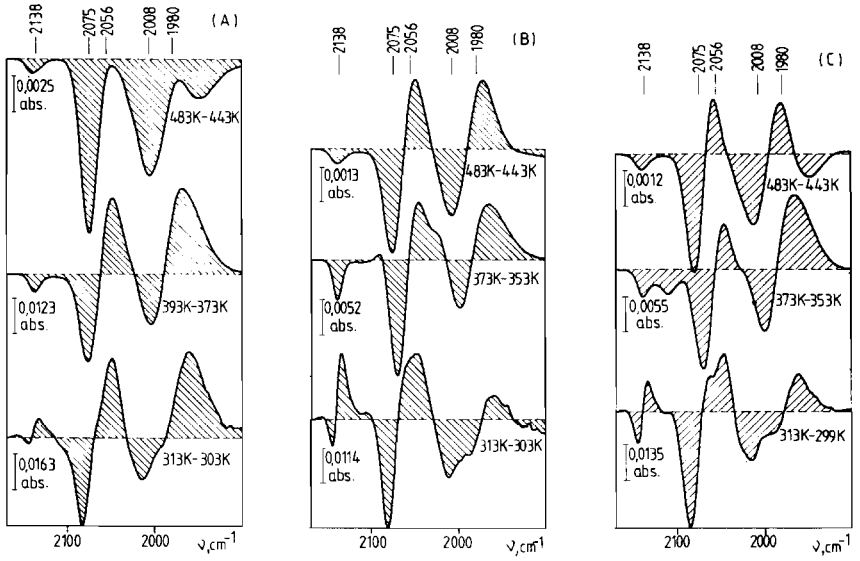

Fig. 6. Characteristic difference spectra of the systems (a) $Ru_3/Al_2O_3/H_2$; (b) $Fe_2Ru/Al_2O_3/H_2$ and (c) $H_2FeRu_3/Al_2O_3/H_2$.

first one from that recorded at the higher temperature; the procedure was consecutively repeated over the whole temperature range. The difference spectra show both positive and negative features. As it follows from the substraction procedure, positive features will be assigned to species forming with increasing temperature and negative features to ones which disappear.

Discussion

The above grouping of the spectra serves for an easier comparison. The main purpose of the present paper is to gain convincing evidences for the analogy between the three systems Ru_3/Al_2O_3, Fe_2Ru/Al_2O_3 and H_2FeRu_3/Al_2O_3.

The spectra recorded during subsequent heating of the samples *in vacuo* are given in Fig. 1(a)–(c). In Fig. 1(a), spectra of the Ru_3/Al_2O_3/vacuum system show five features at wavenumbers 2138(w), ~2075(vs), ~2060(sh), ~2005(s) and ~1980(sh) cm^{-1}. These features seem to remain unchanged over a wide temperature range. At temperatures higher than 403 K the weak peak at 2138 cm^{-1} starts decreasing and, finally, above 573 K the band system rapidly collapses.

The analogous spectra of the system Fe_2Ru/Al_2O_3/vacuum (Fig. 1(b)) essentially shows the same features 2138(w), ~2075(vs), ~2060(sh), ~2005(s) and ~1980(sh) cm^{-1}. The relative intensities of the components, however, are apparently different. The two bands at the wavenumbers 2138(w) and 2075(vs) cm^{-1} are more intense than those in the Ru_3/Al_2O_3/vacuum system. Subsequent heating also results in analogous changes in the spectra.

The behaviour of the system of H_2FeRu_3/Al_2O_3/vacuum (Fig. 1(c)) evidently resembles both spectra described above. The relative intensity of the weak band at 2138 cm^{-1} is between those of Ru_3 and Fe_2Ru. The two shoulders (2060 and 1980 cm^{-1}), however, are more pronounced.

Similar analogies hold for the systems $Ru_3/Al_2O_3/H_2$, $Fe_2Ru/Al_2O_3/H_2$ and $H_2FeRu_3/Al_2O_3/H_2$, that is, the same five bands govern the spectra. In contrast to the samples heated *in vacuo*, in H_2 rather dramatic changes in relative intensities of two pairs of bands at 2075–2005 and 2060–1980 cm^{-1}, are seen. With increasing temperature the intensity of the first pair systematically decreases parallel with the increase of the second pair. The two pairs practically change roles: at low temperatures the second pair (2060–1980 cm^{-1}) is present only as shoulders at the lower wavenumber sides of the first strong pair (2075–2005 cm^{-1}), while at higher temperature their relation is reversed.

As already mentioned in the introduction, for the system of Ru_3/Al_2O_3 the above five bands are known [3–6] and they represent three pairs of bands: A (2140, 2070 cm^{-1}), B (2070, 2001 cm^{-1}) and C (2050, 1970 cm^{-1}) [3–5]. The three pairs may be assigned to the surface species $Ru_A = Ru^{III}(CO)_2$, $Ru_B = Ru^{II}(CO)_2$ and $Ru_C = Ru^0(CO)_2$, respectively [5]. By comparison of the respective spectra of all three systems Ru_3/Al_2O_3, Fe_2Ru/Al_2O_3 and H_2FeRu_3/Al_2O_3 we found that the same five features are characteristic not only of $Ru_3(CO)_{12}$ but for both iron containing catalysts as well and, in a first approximation, there is a comprehensive consistency in the behaviour of these five features. Qualitative inspection of the spectra seems to verify our expectation [2] that bimetallic clusters supported on hydrated

alumina decompose into the same carbonylic surface species like the pure ruthenium cluster and that iron, supposedly oxidized on the surface, does not bond any CO ligand.

However, the spectra of Figs. 1 and 2, besides the above main features, might contain weaker and broader features which are not seen because of the overlap. Furthermore, for the same reasons, even the main five bands (with the exception of that at 2138 cm^{-1}), are not easy to locate in the original absorbance spectra. First of all the positions of the bands located as shoulders are quite uncertain to an extent of about 10–30 cm^{-1}. Finally, information about the shape of the bands is rather insufficient in the standard representation of the spectra.

By derivating the absorbance spectra, spectral features can be enhanced. The first derivative has a local minimum at a shoulder on the high-wavenumber side of a band and a local maximum at a shoulder on the low-wavenumber side. The amplitude/width ratio of the maximum (minimum) is characteristic for the hidden band shape. The second derivative of the spectra represents the accurate location of the absorbance maxima and together with the first derivative is very sensitive to the shape (sharpness) of the bands.

The consistency of both the first derivatives (Fig. 3) and second derivatives (Fig. 4) helps to further elucidate the structure of the spectra. The frequencies for both absorbance maxima and shoulders have proved to be determinable with an accuracy better than ±1 cm^{-1}. Taking into account this precision, all types of bands have proved to be very stable in their location over a wide temperature range.

The highest frequency weak band appears at 2138 ± 0.5 cm^{-1} in the temperature range of 300–443 K for all systems. At higher temperatures, while disappearing, there is a slight shift of 1–2 cm^{-1} toward higher wavenumbers.

The next and generally the most intense peak is found to be located at 2075 ± 0.5 cm^{-1} in the temperature range of 300–583 K, with the exception of the system H_2FeRu_3/Al_2O_3/vacuum where a very small monotonic shift from 2073 to 2078 cm^{-1} has been observed as the temperature increased from 297 K to 573 K. The shape of this band seems to essentially remain unchanged all over. This band has to be assigned to two surface species $Ru^{III}(CO)_2$ and $Ru^{II}(CO)_2$ which supposedly contain two overlapping components one of which makes the pair A with the band at 2138 cm^{-1} while the other one with that at 2008 cm^{-1} (pair of bands B). One may therefore expect these two components to split. Although there is a very slight sign referring to a possible splitting at the second derivative, the coincidence of the two components must be very strict.

The next band, which generally appears as a shoulder around 2055 cm^{-1} in all cases, is slightly shifted towards higher wavenumbers with increasing temperatures. In the system Ru_3/Al_2O_3/vacuum from 2050 to 2055 cm^{-1}, in the system $Ru_3/Al_2O_3/H_2$ from 2050 to 2059 cm^{-1}, in Fe_2Ru/Al_2O_3/vacuum from 2052 to 2053 (practically no shift), in $Fe_2Ru/Al_2O_3/H_2$ from 2049 to 2059 cm^{-1}, in H_2FeRu_3/Al_2O_3/vacuum from 2056 to 2059 and in $H_2FeRu_3/Al_2O_3/H_2$ from 2056 to 2062 cm^{-1}. Notice that the shift is more pronounced in H_2. Despite the shifts of maximum 10 cm^{-1} over a temperature range of ~300 K, they seem to be negligible due to the sensitive mobility of carbonyl stretching frequencies of surface species.

The band at 2008 ± 1 cm^{-1} is widely stable in its location. No systematic change with the increase of temperature can be justified.

The last main feature, the band at 1980 ± 1 cm^{-1} (generally shoulder) is strictly stable in its location.

Although some small broadenings at higher temperatures are present all the five bands proved to preserve their bandwidth over a wide temperature range.

The relative intensities of band pair C (2055–1980 cm^{-1}) show a parallelism. The second derivative spectra also support the hypothesis made for the triad 2138–2075–2008 cm^{-1} as being components of two pairs of bands: 2138–2075 cm^{-1} (pair A) and 2075–2008 cm^{-1} (pair B). For instance, in Ru_3/Al_2O_3/vacuum, above 473 K the band at 2138 cm^{-1} disappears and, in this way, the parallelism between the bands at 2075 and 2008 cm^{-1} is clearly seen (Fig. 4(a)). In addition, we refer to the upper temperature spectra of Fig. 4(b) and 4(c) for supplying the same evidences.

Besides the five main bands, there are some weaker observable features in the derivative spectra. Unfortunately, the first and second derivatives of the spectra are not sensitive to very broad bands. Only relatively sharper bands are supposed to be detectable. Weaker features of medium broadness enhanced by the derivation process are seen at 2110 cm^{-1} in all spectra of Figs 3 and 4 with the exception of the spectra recorded at the highest temperature (573 K). In the same manner, a band at about 2020–2030 cm^{-1} has also been detected.

The all over consistency of the spectra recorded in the temperature range 300–500 K and examined in absorbance and derivative representations, might lead to the conclusion that no events but those involving the five main features take place. However, as shown for the system of Ru_3/Al_2O_3 in our previous paper [6], by quantitative treatment no strict parallelism of the relative intensities of the two band pairs A and B has been found and, as for a rather obvious explanation, we supposed that additional species with additional but hardly detectable spectral features should be considered. Two of them have been found by derivating the spectra as shown above.

TABLE I. Gaussian Parameters and the 'Sharpness' of the Bands (R = Amplitude (A)/Halfwidth (HW)) for Three Characteristic Samples

Sample	Wavenumber (cm^{-1})	A (abs × 100)	HW (cm^{-1})	R (= A/HW)	Assignment
Ru_3/Al_2O_3/vacuum	2136.4	6.90	7.46	0.92	$Ru^{III}(CO)_2$
343 K	2075.9	36.25	7.83	4.63	$Ru^{III}(CO)_2$ and $Ru^{II}(CO)_2$
	2062.0	41.35	15.82	2.61	$Ru^0(CO)_2$
	2044.4	1.51	3.61	0.42	Ru^{II}monocarbonyls
	2005.9	21.65	10.33	2.10	$Ru^{II}(CO)_2$
	1988.6	15.74	45.45	0.35	Ru^0 monocarbonyls
	1983.1	24.13	19.41	1.25	$Ru^0(CO)_2$
H_2FeRu_3/Al_2O_3/vacuum	2138.0	8.02	5.12	1.57	$Ru^{III}(CO)_2$
303 K	2112.5	1.59	30.62	0.05	Ru^{III} monocarbonyls
	2074.0	42.63	9.72	4.38	$Ru^{III}(CO)_2$ and $Ru^{II}(CO)_2$
	2052.9	32.13	10.07	3.19	$Ru^0(CO)_2$
	2006.3	22.50	43.09	0.52	Ru^I monocarbonyls
	2004.1	10.28	8.88	1.16	$Ru^{II}(CO)_2$
	1978.0	24.56	20.01	1.23	$Ru^0(CO)_2$
Fe_2Ru/Al_2O_3/vacuum	2139.2	8.44	4.40	1.92	$Ru^{III}(CO)_2$
298 K	2136.2	3.68	9.98	0.37	Ru^{III} monocarbonyls
	2100.1	1.26	14.84	0.08	
	2073.4	36.13	8.48	4.26	$Ru^{III}(CO)_2$ and $Ru^{II}(CO)_2$
	2059.2	24.27	13.26	1.86	$Ru^0(CO)_2$
	2006.0	10.86	9.28	1.17	$Ru^{II}(CO)_2$
	1986.9	18.35	19.93	0.92	$Ru^0(CO)_2$
	1982.2	7.19	39.03	0.18	Ru^0 monocarbonyls

Besides derivation, there is another very efficient method for enhancing spectral events hidden by the main and/or much sharper features of the spectra. This is the substraction of spectra. In Figs. 5 and 6 for each system, characteristic difference spectra are shown.

The difference spectra of the vacuum systems first of all show that the magnitude of the difference of two spectra recorded at subsequent temperatures, below 493 K, does not exceed 1–10% of the original spectra, which means it is 1–2% at 303–313 K, 5–10% at 443–473 K and 10–20% at 483–573 K. Furthermore, the difference peaks are very broad, the ratios of the amplitudes to half widths $R = A/HW$ are between 0.01–0.05 (in the temperature range of 300–500 K), in comparison to those of $R = 1–4$, characteristic of the five main peaks (see later). Several difference bands (positive and negative) are centered near to the frequencies of the main quintet: 2130–2140, 2080–2060, 2055–2035, 2000–2020 and 1970–1990 cm^{-1}; hence they should be surely considered as surface species analogous to those of $Ru^{III}(CO)_2$, $Ru^{II}(CO)_2$ and $Ru^0(CO)_2$ 'anchored' species. The analogy also holds for their making pairs with parallel intensity behaviours. On the other hand, these bands sensitively increase and decrease with the change of the temperature and in all respects show high mobility. No systematic behaviour, however, in the experiments performed *in vacuo* has been established.

Further very broad positive and negative difference bands develop in the wavenumber ranges of 2150–2100, 2090–2030 and 2020–1930 cm^{-1}, which significantly contribute to the total integrated intensities of the CO stretch bands in the original absorbance spectra. These broad underlying bands will be assigned to monocarbonylic species, where the oxidation state of the ruthenium atoms varies. The highest frequency band belongs to the CO ligands bonded to Ru of highest oxidation state, while that of the lowest frequency to reduced ruthenium atoms. Monocarbonylic species, although interchanging, occur up to very high temperatures (700 K *in vacuo*).

Finally, the less broad bands already detected in the second derivative spectra around 2110 and 2020–2030 cm^{-1} are also involved.

For the samples heated in a H_2 stream the behaviour of the difference spectra seems to be similar, but somewhat more systematic and uniform. Near to room temperature, the intensities of the difference spectra are also similar to those found in vacuum (1–2%). At higher temperatures, however, it quickly increases being at about 10% at 353–373 K and 20%

at 443–483 K. The changes in the spectra are dominated by the decrease of the band pairs A and B and the increase of that of C. Additional weak negative bands are observed at around 2110 and 2030 cm^{-1} at lower temperatures.

As seen, under the five strong bands a large variety of weak bands characteristic of mainly mobile, easily transforming surface species exist and from a spectroscopic point of view, it results in an unstable background that perturbs the attempt to develop quantitatively consistent characterization of the spectra by fitting Gaussians to data points [6]. In spite of this, such a fitting procedure is quite valuable in completing knowledge about the structure of the CO stretching band system. Table I shows the results of the fitting of three representative spectra (Ru_3/Al_2O_3/vacuum/343 K; Fe_2Ru/Al_2O_3/vacuum/298 K and H_2FeRu_3/Al_2O_3/vacuum/303 K). The Gaussian parameters produced by the fitting procedure are in accordance with our expectations. The main bands are quite 'sharp' ($R = A/HW = 1–4$) in contrast to the accompanying bands ($R < 1$). It is very important to notice that there is always a broad band present with the band centre around 2010–1980 cm^{-1}, which has a very large integrated intensity of about 20–30% of the all over integrated intensity of the whole band system.

Finally, in Fig. 7 the all over intensities produced by numerical integration over the frequency range of 2170–1900 cm^{-1} are shown. The integrated intensities are expected to be in strict relation with the total amount of CO on the surface. Till now, we have emphasized the consistency of the data. However, the all over intcgrated intensities also show some interesting features. First of all, the initial part of the curves differ a lot for different clusters. At room temperature the highest intensity occurs for the Ru_3/Al_2O_3/vacuum and H_2 systems. The Fe_2Ru/Al_2O_3/vacuum and H_2 have exactly half intensity and those of H_2FeRu_3/Al_2O_3/vacuum and H_2 a little more than three quarters of it (0.85). However, if the total metal loadings are near identical in all systems as supposed and carbonyls are only bonded to ruthenium atoms, the above intensity ratios are in agreement with the relative content of ruthenium in the respective clusters. With increasing temperature the integrated intensities are constant up to ~500 K or slightly decrease, above 500 K the decrease becomes

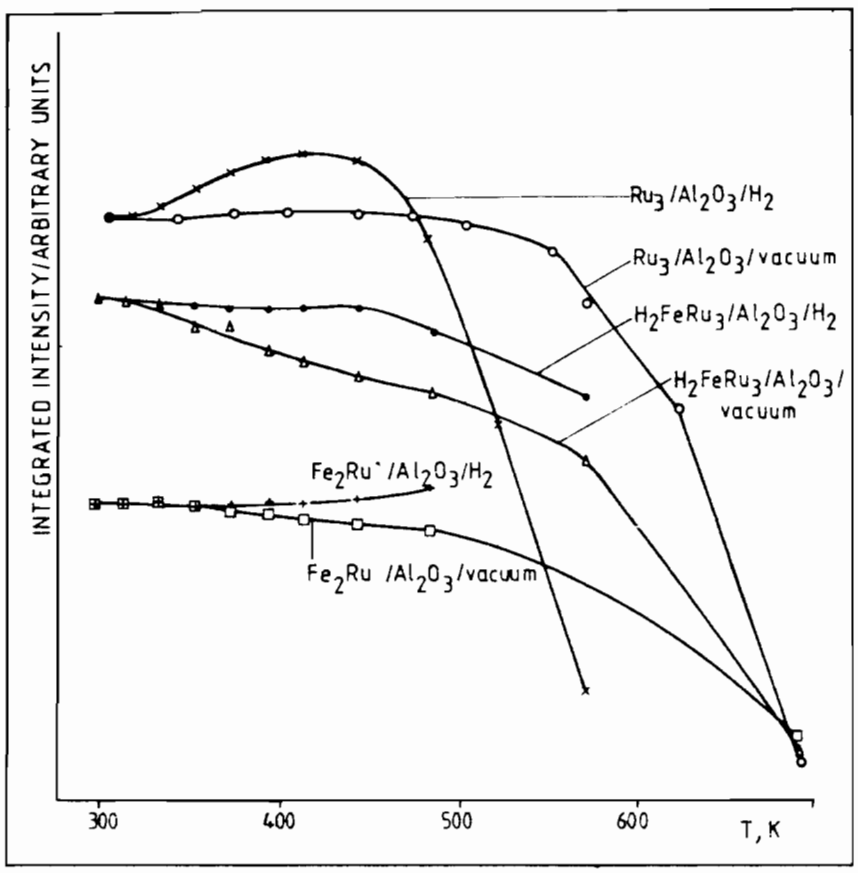

Fig. 7. The change of the integrated intensities of the CO stretching modes, calculated by numerical integration over the frequency range of 2170–1900 cm^{-1}.

faster. The decrease of the intensity in the H_2FeRu_3/Al_2O_3/vacuum system is more pronounced and already begins around 350 K. Generally in H_2 the intensity of carbonyls remains constant up to higher temperatures.

Conclusions

In this paper we thoroughly investigated the details of the spectra of the systems Ru_3/Al_2O_3/vacuum and H_2, Fe_2Ru/Al_2O_3/vacuum and H_2, H_2FeRu_3/Al_2O_3/vacuum and H_2, recorded in a wide temperature range.

(a) We have undoubtedly established that all the above systems show five identical main spectral features at 2138, 2075, 2008 and 1980 cm^{-1}. From this our prediction that iron–ruthenium bimetallic clusters at the end of an interaction with hydrated alumina surface decompose into identical ruthenium carbonylic surface species, like a pure ruthenium cluster, is verified.

(b) The five bands, under the experimental circumstances used in our investigations, proved to be very stable in their frequencies and bandwidths. The bandwidths are rather small, the ratios of amplitude/halfwidth are $R = A/HW = 1-3$, in the same order of magnitude as the ratios $R = A/HW$ calculated for chemisorbed or physisorbed species (see Table I in ref. 8). This means that these bands should be assigned to well defined, molecule-like species.

(c) Taking into account the relative intensities of the five bands and the qualitative parallelisms, the bands can be arranged in three pairs (A: 2138–2075; B: 2075–2008 and C: 2055–1980 cm^{-1}) for all systems, as already suggested in the literature for the Ru_3/Al_2O_3 system [3–5]. Consequently, we extend the assignment introduced by Zecchina *et al.* [5] to the main surface species found in the bimetallic systems, too, as follows: $Ru_A = Ru^{III}(CO)_2$, $Ru_B = Ru^{II}(CO)_2$ and $Ru_C = Ru^0(CO)_2$.

(d) The stability of the frequencies and the sharpness of the five bands supply evidences that Ru_A, Ru_B and Ru_C species are anchored onto rather uniform sites of the surface.

(e) The anchored species Ru_B and Ru_C are stable in a very wide temperature range (300–500 K) and they can be interconverted by oxidation and reduction. Ru_A is less stable (300–400 K).

(f) Besides the anchored species Ru_A, Ru_B and Ru_C, there are analogous surface species present producing very weak (1–5%) and very broad ($R \leqq 0.1$) bands centered near to the main strong bands. These species are mobile (not anchored); they supposedly occupy a large variety of different sites.

(g) The presence of additional underlaying broad ($R \sim 0.5$) bands of rather large integrated intensities indicate the presence of a large amount of monocarbonylic species bonded to ruthenium atoms of different oxidation states. These bands are present up to very high temperatures (700 K *in vacuo*).

(h) The all over integrated intensities of the CO stretching modes indicate that the total amount of carbonyls practically does not decrease below 500 K. In this respect the behaviour of the system $Ru_3/Al_2O_3/H_2$ is exceptional: above 443 K CO dramatically leaves the surface.

References

1 I. Böszörményi and L. Guczi, *Inorg. Chim. Acta, 12,* 5 (1986).
2 I. Böszörményi, S. Dobos, L. Guczi, L. Markó, W. M. Reiff, Z. Schay, L. Takács and A. Vizi-Orosz, 'Proc. 8th Int. Cong. Catal.', Vol. 5, Verlag Chemie, Weinheim, 1984, p. 183.
3 V. L. Kuznetsov, A. Bell and Y. I. Yermakov, *J. Catal., 65,* 374 (1980).
4 H. Knözinger, Y. Zhao, B. Tesche, R. Barth, R. Epstein, B. C. Gates and J. P. Scott, *Faraday Discuss. Chem. Soc., 72,* 53 (1981).
5 (a) A. Zecchina, E. Guglielminotti, A. Bossi and M. Camia, *J. Catal., 74,* 225 (1982); (b) E. Guglielminotti, A. Zecchina, A. Bossi and M. Camia, *J. Catal., 74,* 240 (1982); (c) E. Guglielminotti, A. Zecchina, A. Bossi and M. Camia, *J. Catal., 74,* 252 (1982).
6 S. Dobos, I. Böszörményi, V. Silberer, L. Guczi and J. Mink, *Inorg. Chim. Acta, 96,* L13 (1985).
7 D. B. W. Yawney and F. G. A. Stone, *J. Chem. Soc. A,* 502 (1969).
8 S. Dobos, I. Böszörményi, J. Mink and L. Guczi, *Inorg. Chim. Acta, 120,* 145 (1986).